

PROSPECTS FOR TRIGGERING IN EXPERIMENT PAX AT GSI

A. Kulikov^{a,1}, *G. Macharashvili*^{a,b}

^aJoint Institute for Nuclear Research, Dubna

^bTbilisi State University, Tbilisi, Georgia

In experiment PAX, proposed for the new accelerator complex at GSI, investigations in the field of high-energy spin physics with the use of a polarized antiproton beam are planned. In this paper the possibilities for triggering are considered taking into account the PAX detector properties and a probable configuration of the trigger system is discussed for the first time.

В эксперименте PAX, предложенном для постановки на новом ускорительном комплексе в GSI, планируется проведение исследований в области спиновой физики высоких энергий с использованием поляризованного пучка антипротонов. В данной работе рассматриваются перспективы организации триггера с учетом особенностей детектора PAX и впервые обсуждается возможная конфигурация триггерной системы.

PACS: 07.05.Fb; 07.50.-e; 13.85.-t

INTRODUCTION

The PAX experiment (Polarized Antiproton eXperiments) is a high-energy spin physics project proposed [1] for the future FAIR complex (Facility for Antiproton and Ion Research) [2] at GSI, Darmstadt. A distinctive feature of this experiment is the use of a high-intensity polarized antiproton beam. The method of building polarization in a circulating antiproton beam at the GSI accelerator complex was suggested by the PAX collaboration on the basis of the spin-filtering effect observed in [3] and extensively analyzed in [4]. A high-intensity antiproton beam together with a dedicated detector permits polarization measurements which have never been accessible before. It is worth noting that nowhere, except PAX, such measurements could be possible in the next decade.

In this paper some estimations of trigger possibilities in PAX are done and a probable trigger architecture is discussed. Physics motivation, accelerator layout and detector description are presented here following the experiment Proposal [1].

¹E-mail: kulikov@nusun.jinr.ru

1. PHYSICS GOALS

In order to give an idea about the processes to be detected, let us briefly describe the scope of the PAX physics problems. The main goal of the experiment is the first ever direct measurement of the transversity distribution which describes the transverse quark polarization inside a transversely polarized proton [5]. Transversity is the last missing twist-leading piece of the QCD description of the partonic nucleon structure, and hence the data on transversity would be of fundamental character. The transversity distribution can be obtained via the measurement of the double transverse spin asymmetry A_{TT} in the Drell–Yan production of the lepton pairs in $\bar{p}\uparrow p\uparrow$ interactions.

Other physics items include the study of single-spin asymmetries (SSA) in $\bar{p}\uparrow p$ and $\bar{p}p\uparrow$ interactions, the measurement of the electromagnetic form factors of the proton, the investigation of hard and soft $\bar{p}p$ scattering in polarized and unpolarized cases. Though these tasks were the subject of study in many previous and current experiments¹, there are a lot of hot questions of fundamental importance which are still open and could be answered with PAX. Here we shall not go into details of the physics program motivation and refer to the PAX Proposal [1] and numerous references therein.

2. EXPERIMENT AND DETECTOR LAYOUT

The experiment layout is shown in Fig. 1. Polarized antiprotons are produced by spin filtering [3,4] with an internal polarized hydrogen gas target in a dedicated low-energy (50–200 MeV) polarizer ring (Antiproton Polarizer Ring, APR) after their injection from HESR (High Energy Storage Ring) and deceleration. As the beam polarization is achieved, polarized antiprotons could be accelerated and either hit a fixed target or collide with a proton beam.

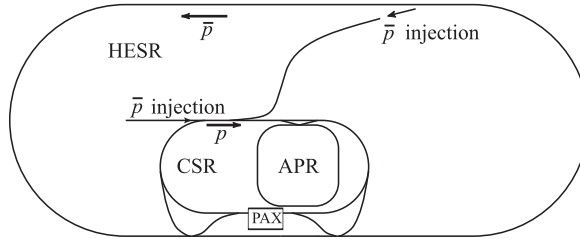


Fig. 1. Scheme of the accelerator complex to be used in the PAX experiment. Placing of APR and CSR outside HESR is also possible

These two versions will be realized at two stages of the experiment. At the first stage (with a fixed target), polarized antiprotons are accelerated to a momentum of 3.5 GeV/c in another ring (Cooler Synchrotron Ring, CSR), similar to COSY [6], and interact with the internal polarized hydrogen target. At the second stage, an asymmetric \bar{p} (15 GeV/c) \times p (3.5 GeV/c) collider is arranged where polarized protons accelerated in CSR collide with polarized antiprotons

¹HERMES at DESY, COMPASS at CERN, experiments at BNL, FNAL and others.

injected back to HESR and accelerated there¹. Note that the APR and CSR rings are dedicated to this experiment while HESR will be in operation independent of the PAX.

In development of the detector concept the following considerations were taken into account. First, from the two options of detection of either e^+e^- or $\mu^+\mu^-$ pairs arising in Drell–Yan processes the electron–positron channel has been chosen for exploration because in the PAX conditions its study involves less complications as argued in [1] (though the $\mu^+\mu^-$ channel is also under study). In order to observe rare reactions, like Drell–Yan processes or $\bar{p}p \rightarrow e^+e^-$ annihilation, the experimental setup should have a large aperture, be able to reliably identify electron–positron pairs of large invariant mass and precisely measure their momenta. Detection of such pairs has to be ensured in a wide kinematic range with a high angular and energy resolution. Strong rejection of hadrons has to be provided in order to identify electrons at the conditions of heavy pion background.

Hadron detection and measurement of their kinematic parameters should also be realized. Finally, it is necessary to measure the energy of γ -quanta from radiative processes and π^0 and η decays.

The present conceptual design of the PAX detector is shown in Fig. 2. Composition and structure of the detector are given here in accordance with [1].

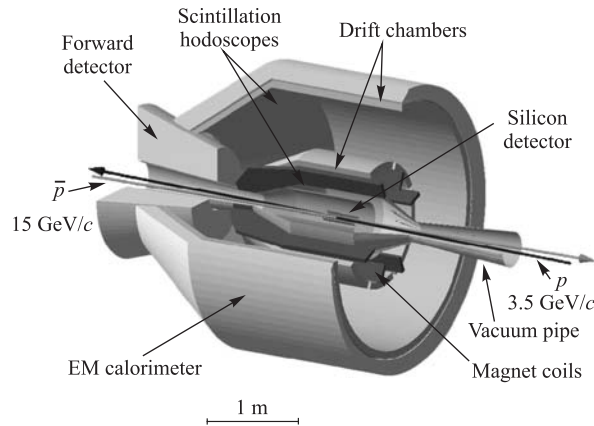


Fig. 2. Conceptual design of the PAX detector (artist's view). Cherenkov detectors between DC1 and DC2 are not shown

The detector is a wide-aperture spectrometer with a magnetic field of toroidal configuration. Its main part is the central detector with an aperture from $\pm 20^\circ$ to $\pm 130^\circ$ in the lab frame. The forward detector (optional) covers the region from about $\pm 8^\circ$ to $\pm 20^\circ$ and supplements the central detector at high-energy measurements, especially for the SSA study.

The central detector includes 3 double-sided silicon microstrip detectors (SiDet) for precise measurement of the primary and secondary vertices, 2 drift chamber (DC) stations, each of 4 signal planes, to measure particle tracks downstream the magnet, a gas Cherenkov counter for

¹Another high-energy mode of operation is also foreseen as a backup option: polarized antiprotons with momentum upgraded to 22 GeV/c impinging on a fixed polarized hydrogen target.

electron identification, an electromagnetic calorimeter (EMCal) to measure particle energies, and scintillation hodoscopes (Hod) used mainly for trigger purposes. The toroid magnet is located between the first scintillation hodoscope plane on the smaller radius side and the inner drift chamber station on the larger radius side, therefore all the detectors are in a field-free region.

The forward detector (less developed at the moment) includes a tracking system similar to that of the central detector and a system for particle identification where the RICH detector is considered as an option.

The detector scheme has not been finalized yet because many aspects of the PAX accelerator complex have to be clarified first. Nevertheless, some preliminary considerations concerning the trigger are possible even at the current stage.

3. GENERAL REQUIREMENTS TO THE TRIGGER SYSTEM IN PAX

In different experiment configurations, the luminosity is expected in the range from $\sim 2 \cdot 10^{30} \text{ cm}^{-2} \cdot \text{c}^{-1}$ for the double polarized asymmetric collider mode to $\sim (1-2) \times 10^{32} \text{ cm}^{-2} \cdot \text{c}^{-1}$ for the unpolarized fixed-target mode. In the latter case, this leads to an interaction rate of several MHz. In conjunction with multiplicity of almost 10, this offers rather tough environment for on-line event selection.

The trigger system has to be flexible enough in order to be easily reconfigured on transition from the fixed-target stage to the collider one. Parallel running of different triggers should be provided for simultaneous accumulation of data for several physics processes and for calibrations as well. Trigger flexibility also permits a free extension of physics program and the study of the processes which are not considered today but could become interesting in forthcoming years.

Electron/hadron separation in Cherenkov counters, total and local energy deposits in EMCal, multiplicity information from the hodoscopes and EMCal, track, momentum and invariant mass reconstruction with the use of the SiDet, DC and EMCal data can be employed for event selection at different trigger levels.

The PAX trigger is supposed to be a two-level system. During the time needed to analyze an event in the first-level trigger logic (T1) the data are preserved in the pipeline memories. Depending on the adopted T1 latency, as many on-line selection criteria as possible should be applied at this level to the data using dedicated hardware processors. More time-consuming operations like, for example, momentum and invariant mass reconstruction, are fulfilled at the second-level trigger stage (T2).

4. SIGNATURES OF PHYSICS PROCESSES

In order to estimate trigger possibilities, let us consider the properties of different physics processes from the point of view of their on-line selection. Here we confine ourselves to only a few main physics items.

Transversity and SSA via Drell-Yan processes. Transversity can be obtained from the measurement of the double transverse spin asymmetry A_{TT} in Drell-Yan processes $\bar{p}\uparrow p\uparrow \rightarrow e^+e^-X$. In PAX, the region of the lepton pair invariant masses $M^2 \simeq 4-100 \text{ GeV}^2$

(combining the fixed-target and the collider modes), which is often considered as the «safe» region for comparison with perturbative QCD predictions has to be explored. As argued in [1], even the region $1.4 \lesssim M^2 \lesssim 3.0 \text{ GeV}^2$ could be used to access transversity.

Measurement of SSA in Drell–Yan processes $\bar{p}\uparrow p \rightarrow e^+e^-X$ or $\bar{p}p\uparrow \rightarrow e^+e^-X$ could shed light on Sivvers function [7] behaviour and, thus, allows better understanding of SSA within QCD.

Triggering for selection of the Drell–Yan pairs can be done via the detection of an electron and a positron with a high invariant mass. High rejection of hadrons (mainly pions) is crucial for this purpose because the Drell–Yan cross section at PAX energies is only few nb compared with the total $\bar{p}p$ cross section of about 50 mb.

Electromagnetic form factors. Measurement of the electromagnetic form factors of the proton is done via the study of antiproton–proton annihilation $\bar{p}p \rightarrow e^+e^-$ in polarized (single and double) and unpolarized modes. Again, electron–positron pairs have to be detected in the presence of high hadron background but the sum of e^+ and e^- energies is fixed in this exclusive reaction allowing better identification of the process.

Antiproton–proton scattering. Elastic $\bar{p}p$ scattering as well as other two-body hadronic final state reactions can be identified using the criteria on coplanarity and momentum and total energy conservation.

Processes with D-meson production. At detection of Drell–Yan pairs the D -meson production is a source of background. At the same time, some other parts of the PAX physics program could be investigated via processes with production of D -mesons. First, the double transverse spin asymmetry A_{TT} , which provides the information on transversity, can be measured in the channel $\bar{p}\uparrow p\uparrow \rightarrow DX$ supplementing the measurements via Drell–Yan process. Another application is the SSA study with D -mesons, $\bar{p}\uparrow p \rightarrow DX$ and $\bar{p}p\uparrow \rightarrow DX$, which allows one to disentangle the Sivvers [7] and Collins [8] mechanisms.

D mesons have short lifetime, the $c\tau$ parameter for D^\pm is equal to 312 μm [9], so they decay close to the interaction point. Therefore, in order to reconstruct decay vertices, a high spatial resolution in the inner part of the detector is required, which is expected to be provided by the silicon strip detector. Due to focusing of the PAX detector on the best electron detection, it is reasonable to search for D -meson events in its semileptonic decay modes with e^+ or e^- emission, the branching ratio of $D^+ \rightarrow e^+X$ being about 17% [9]. Other particles accompanying an electron in this decay should also enter the trigger selection to enrich the collected data sample with D -meson events. The advantageous decay modes are still to be analyzed with a detailed simulation. On the other hand, exclusive hadronic decays of D mesons ($D \rightarrow K2\pi$, $D \rightarrow K3\pi$) could be preferable due to the absence of neutrino in the decay products and hence unambiguous reconstruction of the D -meson invariant mass. Nevertheless, feasibility of use of hadron modes has to be studied because in the current detector scheme reliable on-line separation of pions, kaons and protons is not foreseen.

5. ON-LINE ELECTRON–HADRON SEPARATION

As mentioned above, rejection of hadrons is crucial for efficient Drell–Yan pairs detection in the presence of high pion background. The on-line electron identification is based to a large extent on the Cherenkov counter. The space available for the Cherenkov counter puts limitation on the length of its gas radiator at the level of about 60 cm. This forces us to use

gases with rather large refractive indices, like CO₂ or Freon-12, in order to obtain a reasonably high Cherenkov signal. Pion thresholds for Cherenkov light emission in these gases are

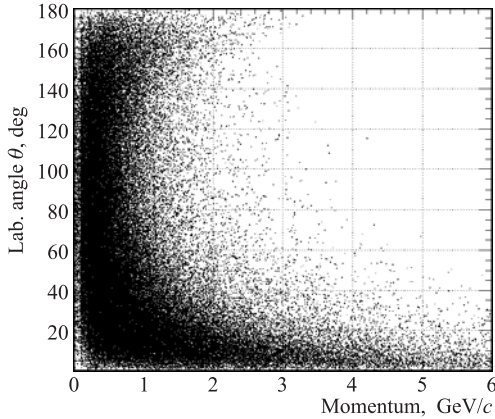


Fig. 3. Plot of charged pion momenta versus the polar angle for the PAX collider mode (simulation with PYTHIA). The detector angular acceptance is $20 < \theta < 130^\circ$

Discrimination of light-emitting pions by Cherenkov amplitudes could help only at energies close to the threshold and at the condition of big response of the counter to electrons.

Other causes for the fake detection of electrons in the Cherenkov counter are gamma-conversions, secondary hadron interactions and decays with emission of electrons upstream or inside the counter.

Therefore, other detectors should also be used at the trigger level for clean electron identification. The complete on-line electron identification algorithm could include, in addition to the presence of the Cherenkov counter signal, a check of associated signals in the hodoscopes and SiDet, measurement of the particle momenta and of the local energy deposits in EMCal, matching of tracks with EMCal hits and a comparison of the measured E and P corresponding to each track. Different steps of this algorithm may be shared between the first and the second trigger levels.

6. TRACKING SYSTEM

Tracking system includes SiDet planes in the inner part of the detector and two stations of drift chambers, DC1 and DC2 (Fig. 4). The magnetic field is localized between two tracking subsystems, so within each of them there is no field (except a weak stray field) and the

¹This is also true for the fixed-target mode because an extensive storage cell will be used in order to increase the target density.

4.873 and 3.003 GeV/ c , respectively. In the E835 experiment the Cherenkov counter [10] (which is referred to in the PAX Proposal) uses the same gases and comparable radiator lengths (72–93 cm for CO₂ and 34–39 cm for Freon-12) and provides the signal ranging from 5 to 20 photoelectrons for different polar angles and azimuthal cells. This signal is generated by the photomultipliers with UV windows with the use of an elaborated light collection system providing 0.85–0.90 (on average) collection efficiency. The latter could hardly be achieved in PAX where the interaction region extends up to 30 cm along the beam¹ (in contrast to a few mm in E835) and hence light focusing is definitely worse.

The main bulk of the pion spectrum in the central detector ($20\text{--}130^\circ$ polar angles) lies in the region below the Cherenkov threshold (see Fig. 3). Nevertheless, the high-momentum tail of the spectrum extends above the threshold.

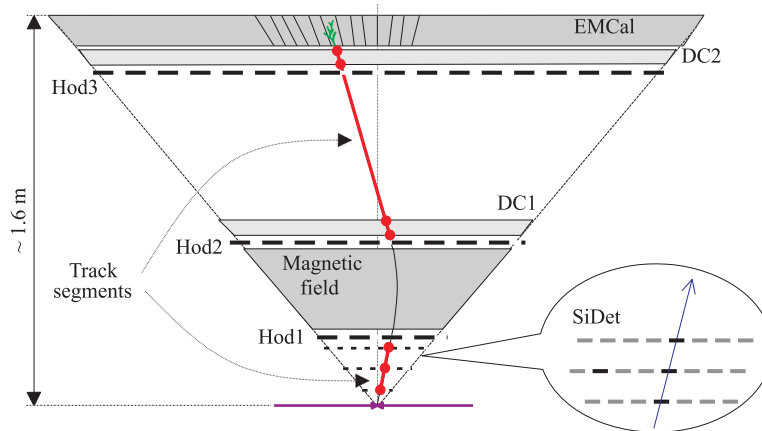


Fig. 4. Detectors used for tracking (central part). Not to scale

trajectory is close to a straight line. Hence, a rather simple algorithm can be used for the search of the track segments, which is feasible at the trigger level. Scintillation hodoscopes Hod1–Hod3 help in the track search defining the region of the track candidates. Linking of segments is also possible, most probably at the second trigger level.

7. TRIGGER ARCHITECTURE

A probable trigger architecture (first briefly discussed in [11]) is shown in Fig. 5. Data from the detectors are digitized directly at the front-end level and then split to the first-level trigger (Level 1) hardware logic and to pipeline memories which preserve the data until the Level 1 decision. Only valid data are transmitted via the pipeline, zero suppression being provided by front-end electronics. Data flow is filtered by the Level 1 decisions and the selected sub-events are stacked in buffer memories. The second-level software trigger (Level 2) receives data from the buffer, builds an event and analyzes it in accordance with the implemented algorithms. A positive decision of Level 2 results in a command to read out the event and record it in the data storage.

Event data for scintillation hodoscopes, Cherenkov counter and EMCal include the coded geographic addresses of detected signals (scintillation counter number, Cherenkov cell number, crystal number¹ in the calorimeter), the signal amplitude and timing information. In drift chambers the numbers of hit wires and measured times are delivered. The SiDet data consist of strip numbers where signals were detected.

Monitoring of the data flow and of trigger decisions is provided at all stages of the event acquisition.

Level 1 Trigger. In order to flexibly construct the trigger, several trigger primitives are built which can be then combined in a needed way to form the Level 1 trigger signal. The

¹At present, the calorimeter type has not been fixed yet: PbWO₄ crystals and alternative options are under study. Further in this paper we use «crystal» to denote an element of the EMCal.

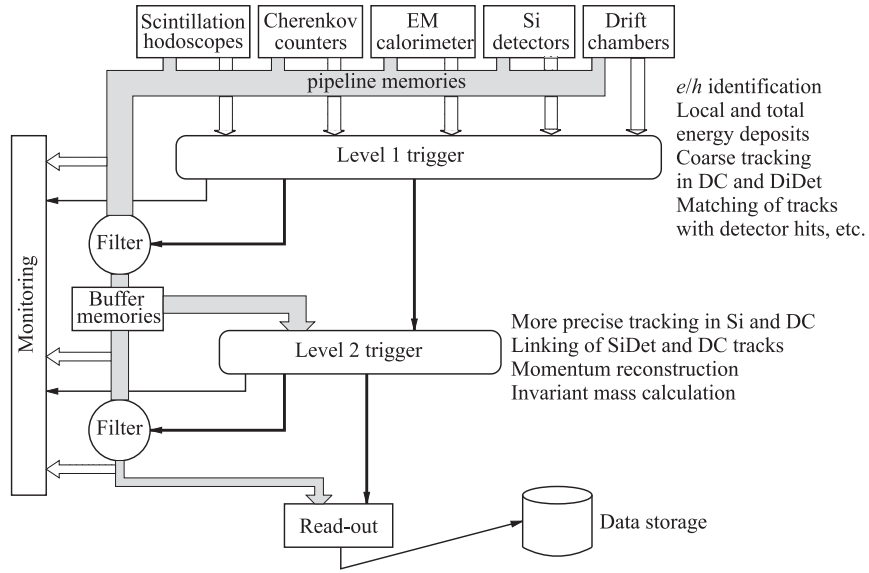


Fig. 5. Probable architecture of the PAX trigger

primitives include a hodoscope trigger HT, a Cherenkov trigger CHT, a drift chamber trigger DCT, calorimeter triggers CALT, CALTOT and a silicon detector trigger ST.

HT is developed when there is a coincidence of signals in the allowed combination of the counters of the hodoscope planes Hod2 and Hod3 (obviously some combinations are kinematically forbidden if the vertex is in the interaction region).

CHT is generated if there is a signal from the Cherenkov counter cell which geometrically matches the particle trajectory as defined by the hodoscope counters.

DCT arises when a straight-line track in the drift chambers is found (at this stage, using only hit wire numbers) associated with the hit hodoscope counters.

CALT is a signal of the calorimeter which means that the cluster signal overshoots the preset threshold. The cluster is defined as a group of neighbor crystals where signals exceed the threshold set for single crystals. Association of a cluster with the track is mandatory when triggering is made on charged particles. When processes with π^0 , η or γ in the final state of the reaction are selected, such an association is not requested. For clusters with the associated track two signals could be provided, CALT(*e*) and CALT(*h*), corresponding to different settings of thresholds for electrons and hadrons. The signal CALT(γ) is formed for a cluster without a close track. In Fig.6 the energy release in the calorimeter is shown for pions, muons and electrons (minimum bias events).

CALTOT is another calorimeter signal arising when the total energy release exceeds the corresponding global threshold. It could be especially useful for triggering on Drell-Yan pairs and annihilation $\bar{p}p \rightarrow e^+e^-$.

ST is developed by coincidence of signals in microstrip silicon detector planes with the use of rather coarse segmentation at this stage.

Note that for fast and efficient construction of the HT, CHT and DCT triggers the scintillation hodoscope plane positioned just in front of the DC1 station is very helpful. In this case, a straight-line trajectory between the two hodoscope planes downstream the magnetic field region allows fast and simple algorithms to be used. That differs from the PAX Proposal layout where the first of the two available hodoscope planes is placed upstream of the toroid magnet and hence the particle trajectory between the hodoscopes is not a straight line. Simple replacement of the first plane is not a very good solution because in its «old» position it serves for the track search in SiDet. So, we propose to supplement the detector with an additional hodoscope plane (Hod2 in Fig. 4) in front of the DC1 station.

The built trigger primitives can be combined in order to select candidates for electrons, hadrons and gammas. For example, the complete selection formula for the electron is $HT \cdot CHT \cdot DCT \cdot CALT(e) \cdot ST$. Gamma conversions are essentially suppressed here due to the request of hits in SiDet and Hod2 mandatory for ST and HT triggers. Depending on experimental conditions, hardness of selection may be varied by exclusion of some primitives from the coincidences or by a change of parameters at formation of the primitives. This permits finding a compromise between the trigger rate and efficiency.

Once individual particles are classified, their combinations like e^+e^- , e^+e^-X , h^+h^- and others can be arranged at Level 1. The global Level 1 trigger is a logical sum of all activated trigger modes after their individual prescaling (when appropriate).

The apparatus of the Level 1 trigger logic will be based on the use of the FPGAs (Field Programmable Gate Array) and look-up memories which nowadays and in the forthcoming decade seem to be the best hardware technology for flexible trigger applications. Parameters defining correlations between hits in the detectors for useful events will be obtained from simulation of the processes in the conditions of the precise setup geometry and will be used for programming of the hardware logic elements.

The Level 1 trigger will have a fixed latency. The experience of other experiments [12] shows that the latency of a few μs (and hence the needed pipeline memory depth) is sufficient for all the above operations.

Once a positive Level 1 decision is taken, detector data for the selected event are put to the buffer memories waiting for analysis by the Level 2 stage. Some additional information, obtained at the Level 1 acquisition, is written to the buffer helping to minimize further computing operations: regions of interest in SiDet determined by the ST algorithm, DC wire numbers which enter the track found by DCT, etc.

Level 2 Trigger. Further event selection is provided by the software Level 2 trigger. In order to minimize the processing time for tracking, the pointers provided by Level 1 are used. The Level 2 selection may include:

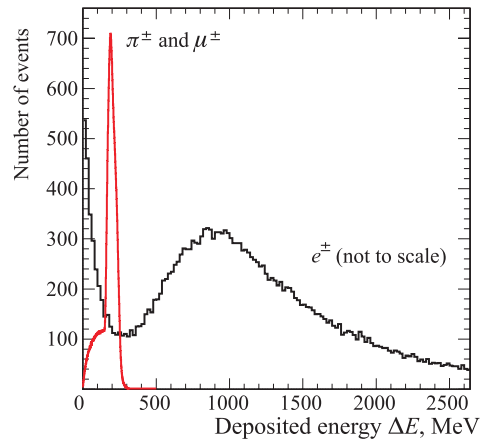


Fig. 6. Simulated energy deposits of different particles in the electromagnetic calorimeter

- precise tracking in DC using drift times and applying χ^2 cut. Precise track reconstruction is made here for wire numbers belonging to the tracks as defined by the Level 1 logic;
- search for track segments in SiDet. The search is fulfilled in regions of interest marked at Level 1 when the subtrigger ST was developed;
- linking of track segments in DC and SiDet;
- reconstruction of the vertex and a cut on the vertex coordinates;
- momentum reconstruction with the use of the track parameters and the magnetic field configuration;
- improvement of electron identification by comparison of the reconstructed momentum with the energy measured in EMCal;
- invariant mass reconstruction.

In different trigger options some of the above steps may be skipped.

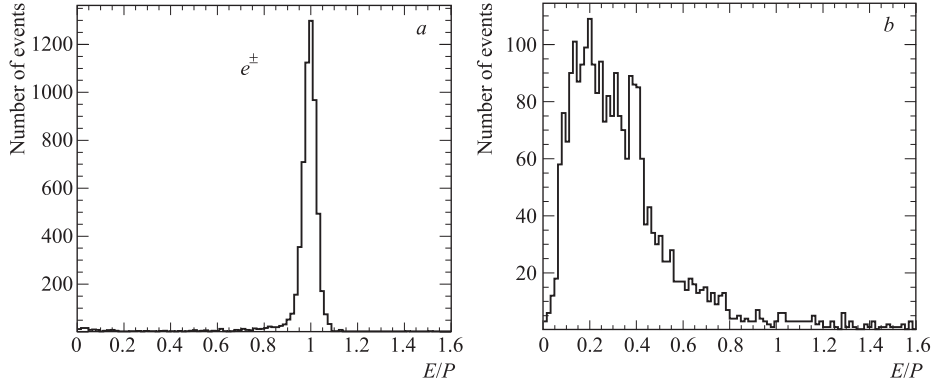


Fig. 7. Ratio of the energy E to momentum P expected for electrons from the Drell–Yan pairs (a) and charged background (b)

In Fig. 7 the expected ratio of the energy E to momentum P measured in the PAX detector is shown for the Drell–Yan electrons and charged background. It is seen that with the cut $E/P = 1.0 \pm 0.1$ essential background suppression, about 50, could be obtained.

CONCLUSIONS

The presented ideas about the possible structure of the PAX trigger system may be considered as a starting point for deeper study of this subject. As soon as more progress is achieved in finalizing of the accelerator complex design and the detector structure, detailed simulations of the trigger should start using a more precise geometry, real granularity of sub-detectors taking into account the background induced in the toroid magnet and other constructive elements of the setup. The final trigger architecture will be developed together with the data acquisition system when a reliable estimation of the sub-detector rates, background level and event topologies is obtained.

REFERENCES

1. *PAX collab.* Antiproton–Proton Scattering Experiments with Polarization. Technical Proposal. hep-ex/0505054 v1. 2005.
2. *Äystö L. et al.* An International Accelerator Facility for Beams of Ions and Antiprotons. Conceptual Design Report. GSI, 2001.
3. *Rathmann F. et al.* New Method to Polarize Protons in a Storage Ring and Implications to Polarize Antiprotons // *Phys. Rev. Lett.* 1993. V. 71, No. 9. P. 1379–1381.
4. *Meyer H. O.* // *Phys. Rev. E.* 1994. V. 50, No. 2. P. 1485–1490;
Horowitz C. J., Meyer H. O. // *Phys. Rev. Lett.* 1994. V. 72, No. 25. P. 3981–3984;
Milstein A. I., Strakhovenko V. M. // *Phys. Rev. E.* 2005. V. 72. P. 066503-1–066503-5;
Nikolaev N. N., Pavlov F. F. hep-ph/0512051;
Nikolaev N. N., Pavlov F. F. hep-ph/0601184.
For the recent 2006 review see: Update of Technical Proposal for PAX, Appendix G. http://www.fz-juelich.de/ikp/pax/news/news_files/TP_Add_update.pdf
5. For review on the transverse spin structure of the proton, see: *Barone V., Drago A., Ratcliffe P.* Transverse Polarization of Quarks in Hadrons // *Phys. Rep.* 2002. V. 359, No. 1–2. P. 1–168.
6. *Maier R.* Cooler Synchrotron COSY – Performance and Perspectives // *Nucl. Instr. Meth. A.* 1997. V. 390, No. 1–2. P. 1–8.
7. *Sivers D.* Single-Spin Production Asymmetries from the Hard Scattering of Pointlike Constituents // *Phys. Rev. D.* 1990. V. 41, No. 1. P. 83–90; Hard-Scattering Scaling Laws for Single-Spin Production Asymmetries // *Phys. Rev. D.* 1991. V. 43, No. 1. P. 261–263.
8. *Collins J. C.* Fragmentation of Transversely Polarized Quarks Probed in Transverse Momentum Distributions // *Nucl. Phys. B.* 1993. V. 396, No. 1. P. 161–182.
9. Particle Data Group. Available from <http://pdg.lbl.gov>
10. *Bagnasco S. et al.* The Threshold Gas Cherenkov Counter of Charmonium Experiment 835 at Fermilab // *Nucl. Instr. Meth. A.* 1999. V. 424, No. 2–3. P. 304–320.
11. *Kulikov A.* Triggering at Storage Rings // *Proc. of the 6th Intern. Conf. on Nuclear Physics at Storage Rings (STOR1'05)*, Jülich–Bonn, Germany, May 23–26, 2005; *Matter and Materials.* V. 30, P. 394–397.
12. See, for example: *Adler S. S. et al.* PHENIX On-Line Systems // *Nucl. Instr. Meth. A.* 2003. V. 499, No. 2–3. P. 560–592;
Aubert B. et al. The BABAR Detector // *Nucl. Instr. Meth. A.* 2002. V. 479, No. 1. P. 1–116;
Gerndt E. K. E. et al. HERA-B: Trigger System // *Nucl. Instr. Meth. A.* 2000. V. 446, No. 1–2. P. 264–273.

Received on April 26, 2006.